# Spectral Efficiency Maximization in Aerial STAR-RIS-Assisted Massive MIMO-RSMA Networks

Ridho Hendra Yoga Perdana\*, and Taejoon Kim\*

\*School of Information and Communication Engineering, Chungbuk National University, Cheongju 28644, South Korea Emails: \*mail.rhyp@gmail.com, \*ktjcc@chungbuk.ac.kr

Abstract—In this paper, we study a spectral efficiency (SE) maximization problem in downlink aerial simultaneously transmitting and reflecting (STAR)-reconfigurable intelligent surface (RIS)-assisted massive multiple-input multiple-output (mMIMO)rate-splitting multiple access (RSMA) networks. The formulated problem belongs to the non-convex mixed-integer class due to the maximum allowable portion of common SE, power budget limitation at the flying-base station (F-BS) and the discrete phase shift at the flying-STAR-RIS (F-SR), which is difficult to solve optimally. To tackle this problem, the formulated problem is relaxed and then decoupled into a phase-shift and a beamforming subproblem, and then solved alternately. A bisection search method is applied to address the phase shift sub-optimization problem, while the inner approximation (IA) technique is utilized to solve the beamforming sub-problem by transforming the original non-convex formulation into more tractable forms. Simulation results show that the proposed scheme can improve SE performance. Besides, the impact of the number of F-BS antennas and F-SR elements on the considered system is also evaluated.

*Index Terms*—mMIMO, non-convex optimization, RSMA, spectral efficiency, phase shift, STAR-RIS.

# I. INTRODUCTION

High spectral efficiency (SE) and energy efficiency (EE) is a critical performance metric in next-generation wireless communication networks [1], [2]. To achieve high SE, manage interference effectively, and support high-capacity communication in dense user environments, massive multipleinput multiple-output (mMIMO), non-orthogonal multiple access (NOMA) and rate-splitting multiple access (RSMA) are widely adopted [3]–[5]. However, when obstacles are present between the base station (BS) and users, the quality of the received signal can deteriorate significantly due to blockage and non-line-of-sight propagation. To overcome this problem, the use of simultaneously transmitting and reflecting reconfigurable intelligent surfaces (STAR-RIS) has emerged as a promising solution [6], [7]. Unlike conventional RIS that only reflects signals, STAR-RIS enables both transmission and reflection, thereby extending coverage and enhancing signal quality for users located on both sides of the surface [8]. This dual-functionality makes STAR-RIS particularly effective in mitigating blockage effects and improving signal reception in complex propagation environments. Additionally, applying the RSMA method can also increase SE performance since it can manage the interference by splitting the message into a

common and a private stream [9]. Moreover, as the scale of mMIMO and STAR-RIS systems increases, the complexity of resource allocation and configuration also grows, posing new challenges for system design and optimization.

Previous studies have independently investigated RSMA and STAR-RIS within mMIMO systems. However, beyond-5G networks demand their integrated deployment, which, despite offering substantial performance benefits, introduces significant challenges in interference mitigation, resource allocation, and system complexity. The joint optimization of SE for user equipment (UE) becomes particularly challenging due to the large-scale nature of BS antennas and STAR-RIS elements, making the problem highly complex and difficult to solve. The main contributions of the paper are as follows:

- A spectral efficiency maximization (SEM) problem is formulated by jointly linear precoding vector and the discrete phase shift matrix for reflection/transmission at the flying-STAR-RIS in massive MIMO-RSMA systems. This problem belongs to the mixed integer programming class, which is challenging to solve.
- To tackle the formulated problem, the discrete phase shift is relaxed into a continuous form and decomposed into beamforming and phase shift sub-problems. A bisectionbased search algorithm is employed to tackle the phase shift sub-problem, while the beamforming sub-problem is addressed using the inner approximation (IA) method.
- Simulation results show that the considered system achieves better SE performance than mMIMO-RSMA without flying-STAR-RIS.

*Notation*: a,  $\mathbf{A}$ ,  $\mathbf{A}$  denote the scalar, vectors, and matrices, respectively.  $\operatorname{diag}(\mathbf{A})$ ,  $|\cdot|$ ,  $(\cdot)^*$  is the diagonal matrix, absolute of values, complex conjugate, respectively.  $\mathfrak{R}$  and  $\mathbb{C}$  represent real part and complex numbers, respectively.

## II. SYSTEM MODEL

The downlink multi-user STAR-RIS-assisted mMIMO-RSMA network is considered, where a flying-base station (F-BS) is deployed to serve a ground user 1  $(GU_1)$  and a ground user 2  $(GU_2)$  via flying-STAR-RIS (F-SR) using RSMA which located in the 3D Cartesian coordinates, as shown in Fig. 1. The F-BS is equipped with  $M_S>1$  antennas, and both users are equipped with a single antenna, while F-SR is equipped with  $L=L^{rf}+L^{tf}$  elements,

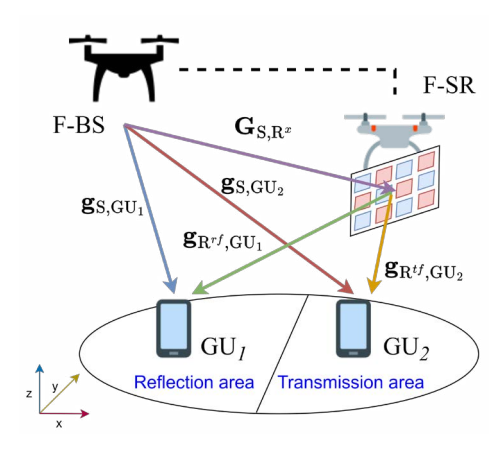


Fig. 1. The proposed system model of STAR-RIS-assisted mMIMO-RSMA networks.

where  $L^{rf}$  and  $L^{tf}$  are reflecting and transmission parts, reflectively. Moreover, the F-SR operates in mode switching (MS) mode, as it can serve both users simultaneously [10].

We assume that both F-BS and users have perfect knowledge of the channel state information (CSI), enabling the use of zero-forcing transmission under high signal-to-interference-plus-noise ratio (SINR) conditions. The F-BS is also responsible for determining the two-phase shifts reflection and transmission at the F-SR. In reflection mode, the desired signal is reflected solely through the  $L^{rf}$  element without experiencing channel attenuation, while in transmission mode, the signal passes through the  $L_{tf}$  element without reflection. To emphasize the phase-shift configuration, we further assume ideal reflection and transmission amplitudes, i.e.,  $\lambda = \lambda^{rf} = \lambda^{tf} = 1$ .

## A. STAR-RIS-assisted mMIMO

According to RSMA transmission, the F-BS transmits common and private messages. The common message is encoded and encapsulated into the common stream  $\zeta^c$ , while the private message of each user is encoded into a private stream  $\zeta_1^p$  and  $\zeta_2^p$  independently. The stream vector  $\boldsymbol{\zeta} = [\zeta^c, \zeta_1^p, \zeta_2^p]^T$  is lineary precoded using the beamformer  $\mathbf{w} = [\mathbf{w}^c, \mathbf{w}_1^p, \mathbf{w}_2^p] \in \mathbb{C}^{M_5 \times 3}$ . Thus, the transmit signal from F-BS to both users  $(GU_1 \text{ and } GU_2)$  can be expressed as

$$\mathbf{s} = \mathbf{w}^c \zeta^c + \mathbf{w}_1^p \zeta_1^p + \mathbf{w}_2^c \zeta_2^p. \tag{1}$$

The channels between F-BS and  $GU_1$  and  $GU_2$ , denoted as  $\hat{\mathbf{g}}_{SU_1} \in \mathbb{C}^{1 \times M_S}$  and  $\hat{\mathbf{g}}_{SU_2} \in \mathbb{C}^{1 \times M_S}$ , can be expressed, respectively, as

$$\hat{\mathbf{g}}_{SU_1}(\mathbf{\Phi}) = \mathbf{g}_{S,GU_1} + \mathbf{G}_{S,R^{rf}} \mathbf{\Phi} \mathbf{g}_{R^{rf},GU_1}, \tag{2}$$

$$\hat{\mathbf{g}}_{\mathrm{SU}_2}(\mathbf{\Psi}) = \mathbf{g}_{\mathrm{S},\mathrm{GU}_2} + \mathbf{G}_{\mathrm{S},\mathrm{R}^{tf}} \mathbf{\Psi} \mathbf{g}_{\mathrm{R}^{tf},\mathrm{GU}_2}, \tag{3}$$

where  $\mathbf{g}_{S,GU_1} \in \mathbb{C}^{1 \times M_S}$ ,  $\mathbf{G}_{S,R^{rf}} \in \mathbb{C}^{L^{rf} \times M_S}$ ,  $\mathbf{g}_{R^{rf},GU_1} \in \mathbb{C}^{1 \times L^{rf}}$ ,  $\mathbf{g}_{S,GU_2} \in \mathbb{C}^{1 \times M_S}$ ,  $\mathbf{G}_{S,R^{tf}} \in \mathbb{C}^{L^{tf} \times M_S}$ , and  $\mathbf{g}_{R^{tf},GU_2} \in \mathbb{C}^{1 \times L^{tf}}$ , denote the channels from F-BS to  $GU_1$ , from F-BS to F-SR with reflection part, from F-SR with reflection part to  $GU_1$ , from F-BS to  $GU_2$ , from F-BS to F-SR with transmission part, from F-SR

with transmission part to  $GU_2$ , respectively. The reflection and transmission property of F - SR is determined by

$$\mathbf{\Phi} = \operatorname{diag}\left(\lambda_1^{rf} e^{j\phi_1}, ..., \lambda_L^{rf} e^{j\phi_{L^{rf}}}\right),\tag{4}$$

$$\mathbf{\Psi} = \operatorname{diag}\left(\lambda_1^{tf} e^{j\psi_1}, ..., \lambda_L^{rf} e^{j\psi_{L^{tf}}}\right),\tag{5}$$

where  $\phi_{l^rf} \in (0, 2\pi]$  and  $\psi_{l^tf} \in (0, 2\pi]$  denote the phase shift of reflection and transmission of the l-th element of the F-SR. We set the phase shift of F-SR at each element is discrete values with resolution  $\delta=2^r$ , where r is phase shift quantize levels [11]. Thus, a set of discrete phase shift values at each element of F-SR can be expressed as

$$\mathcal{D} = \{0, \mathcal{A}\theta, \cdots, (\delta - 1)\mathcal{A}\theta\},\tag{6}$$

where  $\mathcal{A} \in \{\Phi, \Psi\}$ ,  $\theta \in \{\phi, \psi\}$ ,  $\mathcal{A}\theta = 2\pi/\delta$ . The channel coefficient matrix is given by  $\mathbf{G} = \sqrt{g}_{xy}\tilde{\mathbf{G}}$ ,  $\tilde{\mathbf{G}} \in \{\mathbf{G}_{\mathrm{S},\mathrm{R}^{rf}},\mathbf{G}_{\mathrm{S},\mathrm{R}^{tf}}\}$ , where  $g_{xy}$  represents the large-scale fading from to with  $\in \{\mathrm{F}-\mathrm{BS},\mathrm{F}-\mathrm{SR}\}$  and  $\in \{\mathrm{F}-\mathrm{SR},\mathrm{GU}_1,\mathrm{GU}_2\}$ , while  $\tilde{\mathbf{G}}$  is the small-scale fading. While the channel coefficient vector is given by  $\mathbf{g} = \sqrt{g}\tilde{\mathbf{g}}$ ,  $\tilde{\mathbf{g}} \in \{\mathbf{g}_{\mathrm{S},\mathrm{GU}_1},\mathbf{g}_{\mathrm{R}^{rf},\mathrm{GU}_1},\mathbf{g}_{\mathrm{S},\mathrm{GU}_2},\mathbf{g}_{\mathrm{R}^{rf},\mathrm{GU}_2}\}$ , where  $\tilde{\mathbf{g}}$  is the small-scale fading.

The received message at  $\mathrm{GU}_1$  and  $\mathrm{GU}_2$  can be expressed, respectively, as

$$y_1 = \hat{\mathbf{g}}_{SU_1}(\boldsymbol{\Phi})\mathbf{w}^c \zeta^c + \hat{\mathbf{g}}_{SU_1}(\boldsymbol{\Phi})\mathbf{w}_1^p \zeta_1^p + \hat{\mathbf{g}}_{SU_1}(\boldsymbol{\Phi})\mathbf{w}_2^c \zeta_2^p + n_1,$$
(7)

$$y_2 = \hat{\mathbf{g}}_{SU_2}(\boldsymbol{\Psi})\mathbf{w}^c \zeta^c + \hat{\mathbf{g}}_{SU_2}(\boldsymbol{\Psi})\mathbf{w}_1^p \zeta_1^p + \hat{\mathbf{g}}_{SU_2}(\boldsymbol{\Psi})\mathbf{w}_2^c \zeta_2^p + n_2,$$
(8)

where  $n_1 \sim \mathcal{CN}(0, \sigma_1^2)$  and  $n_2 \sim \mathcal{CN}(0, \sigma_2^2)$  represent the additive white noises at  $GU_1$  and  $GU_2$ , respectively.

Based on the RSMA principle, the SINR to decode the common message at  $\mathrm{GU}_1$  and  $\mathrm{GU}_2$  can be expressed, respectively, as

$$\gamma_1^c(\mathbf{w}, \mathbf{\Phi}) = \frac{|\hat{\mathbf{g}}_{SU_1}^H(\mathbf{\Phi}) \mathbf{w}^c|^2}{|\hat{\mathbf{g}}_{SU_1}^H(\mathbf{\Phi}) \mathbf{w}_1^p|^2 + |\hat{\mathbf{g}}_{SU_1}^H(\mathbf{\Phi}) \mathbf{w}_2^p|^2 + \sigma_1^2}, \quad (9)$$

$$\gamma_2^c(\mathbf{w}, \mathbf{\Psi}) = \frac{|\hat{\mathbf{g}}_{SU_2}^H(\mathbf{\Phi})\mathbf{w}^c|^2}{|\hat{\mathbf{g}}_{SU_2}^H(\mathbf{\Phi})\mathbf{w}_1^p|^2 + |\hat{\mathbf{g}}_{SU_2}^H(\mathbf{\Phi})\mathbf{w}_2^p|^2 + \sigma_2^2}, \quad (10)$$

while the SINR to decode the private message at  $\mathrm{GU}_1$  and  $\mathrm{GU}_2$  can be expressed, respectively, as

$$\gamma_1^p(\mathbf{w}, \mathbf{\Phi}) = \frac{|\hat{\mathbf{g}}_{SU_1}(\mathbf{\Phi})\mathbf{w}_1^p|^2}{|\hat{\mathbf{g}}_{SU_1}(\mathbf{\Phi})\mathbf{w}_2^p|^2 + \sigma_1^2},$$
(11)

$$\gamma_2^p(\mathbf{w}, \mathbf{\Psi}) = \frac{|\hat{\mathbf{g}}_{SU_2}(\mathbf{\Phi})\mathbf{w}_2^p|^2}{|\hat{\mathbf{g}}_{SU_2}(\mathbf{\Phi})\mathbf{w}_1^p|^2 + \sigma_2^2}.$$
 (12)

The achievable SE of  $\mathrm{GU}_1$  and  $\mathrm{GU}_2$  for common and private messages in nat/sec/Hz can be written, respectively, as

$$_{1}^{c}(\mathbf{w}, \mathbf{\Phi}) = \ln(1 + \gamma_{1}^{c}(\mathbf{w}, \mathbf{\Phi})), \tag{13}$$

$$_{1}^{p}(\mathbf{w}, \mathbf{\Phi}) = \ln(1 + \gamma_{1}^{p}(\mathbf{w}, \mathbf{\Phi})), \tag{14}$$

$$_{2}^{c}(\mathbf{w}, \mathbf{\Psi}) = \ln(1 + \gamma_{2}^{c}(\mathbf{w}, \mathbf{\Psi})), \tag{15}$$

$$_{2}^{p}(\mathbf{w}, \mathbf{\Psi}) = \ln(1 + \gamma_{2}^{p}(\mathbf{w}, \mathbf{\Psi})). \tag{16}$$

Since the achievable common SE is shared among all users, the total achievable common SE shall not exceed  $^{c}=$ 

 $\min\{ \begin{array}{ccc} c & c \\ 1 & c \end{array} \}$  and we have  $\begin{array}{ccc} c + c \\ 1 & c \end{array} \le \begin{array}{ccc} c \end{array}$ . Thus, the total achievable SE of  $\mathrm{GU}_1$  and  $\mathrm{GU}_2$  can be written, respectively, as

$$_{1}(\mathbf{w}, \mathbf{\Phi}) = {}^{c}_{1}(\mathbf{w}, \mathbf{\Phi}) + {}^{p}_{1}(\mathbf{w}, \mathbf{\Phi}),$$
 (17)

$$_{2}(\mathbf{w}, \mathbf{\Psi}) = {}^{c}_{2}(\mathbf{w}, \mathbf{\Psi}) + {}^{p}_{2}(\mathbf{w}, \mathbf{\Psi}).$$
 (18)

#### B. Problem Formulation

The main goal of this paper is to maximize SE in the network subject to the maximum transmit power at F-BS,  $\bar{P}_{F-BS}$ , common SE constraint  $^c$ , and discrete phase shift at F-SR by optimizing the precoding vector  $\mathbf{w}$  and phase shift reflection  $\mathbf{\Phi}$  and transmission  $\mathbf{\Psi}$  at F-SR which can be formulated as

$$\max_{\mathbf{w}, \mathbf{\Phi}, \mathbf{\Psi}} \quad \text{SEM} \triangleq \quad {}_{1}(\mathbf{w}, \mathbf{\Phi}) + \quad {}_{2}(\mathbf{w}, \mathbf{\Psi})$$
 (19a)

s.t. 
$$\begin{pmatrix} c \\ 1 \end{pmatrix} + \begin{pmatrix} c \\ 2 \end{pmatrix} \leq \begin{pmatrix} c \\ c \end{pmatrix}$$
, (19b)

$$_{1}(\mathbf{w},\mathbf{\Phi}) \geq _{1}^{-},$$
 (19c)

$$_{2}(\mathbf{w}, \mathbf{\Psi}) \geq _{2},$$
 (19d)

$$||\mathbf{w}^c||^2 + ||\mathbf{w}_1^p||^2 + ||\mathbf{w}_2^p||^2 \le \bar{P}_{BS},$$
 (19e)

$$e^{j\phi_1} \in \mathcal{D}, \ e^{j\psi_1} \in \mathcal{D}$$
 (19f)

where constrain (19b) defines the maximum allowable portion of common SE. Constraints (19c) and (19d) ensure that the total SE at each ground user meets or exceeds the minimum required threshold. Constraint (19e) enforces the power budget limitation at the F-BS, while constraint (19f) enforces the discrete nature of the F-SR phase shift. The formulated problem in (19) is evidently non-convex and involves mixed-integer constraints, which poses significant challenges for solving the global optimum.

## III. THE PROPOSED SEM ALGORITHM

It is important to note that the problem (19) is a non-convex fractional optimization problem with mixed-integer constraints. To make it more tractable, the integer phase shift is first relaxed into a continuous form. Thus, problem (19) can be re-written as

$$\max_{\mathbf{w}, \mathbf{\Phi}, \mathbf{W}} \quad \text{SEM} \triangleq \quad {}_{1}(\mathbf{w}, \mathbf{\Phi}) + \quad {}_{2}(\mathbf{w}, \mathbf{\Psi})$$
 (20a)

s.t. 
$$\phi_{l^{rf}} \in [0, 2\pi], \ \psi_{l^{tf}} \in [0, 2\pi],$$
 (20b)

The problem (20) is fractional form with non-convex constraints. The effective way to solve this problem is to decompose it into beamforming and phase shift sub-problems, which are solved sequentially.

# A. Phase shift Optimization Sub-Problem

Now we start to solve the phase shift optimization sub-problem. By fixing the beamforming vector variable in problem (20), yielding

$$\max_{\mathbf{\Phi}, \mathbf{\Psi}} \quad \text{SEM} \triangleq \quad {}_{1}(\mathbf{\Phi}) + \quad {}_{2}(\mathbf{\Psi})$$
 (21a)

Noted that the objective function (21a) is concave, while the constraint (20b) is linear. Subsequently, a Bisection Search-based algorithm is proposed to efficiently solve this problem.

#### B. Beamforming Optimization Sub-Problem

Now we are in the position to solve the beamforming optimization sub-problem after achieving optimal phase shift. With the optimal phase shift obtained, the original problem (20) can be written as

$$\max_{\mathbf{w}} \quad \text{SEM} \triangleq \quad {}_{1}(\mathbf{w}) + \quad {}_{2}(\mathbf{w}) \tag{22a}$$

Noted that the objective function (22) is concave while constraint (22b) is non-convex. To facilitate tractability, we introduce a set of auxiliary variables  $\boldsymbol{\xi} \triangleq \{\xi^c, \xi_1^p, \xi_2^p\}$  and  $\boldsymbol{v} \triangleq \{v_1, v_2\}$  where  $\xi^c$ ,  $\xi_1^p$ , and  $\xi_2^p$  represent the soft data rates of common messsage, and the private message for  $\mathrm{GU}_1$  and  $\mathrm{GU}_2$ , respectively, while  $v_1$  and  $v_2$  denote the soft SINRs for  $\mathrm{GU}_1$  and  $\mathrm{GU}_2$ , respectively. We then reformulate problem (22) into an equivalent non-convex form that is more tractable. Following the inner approximation (IA) method, the problem (22) can be approximated at the  $(\kappa+1)$ -th iteration as follows:

$$\max_{\mathbf{w}, \boldsymbol{\xi}, \boldsymbol{v}} \quad \text{SEM} \triangleq v_1 + v_2 \tag{23a}$$

s.t. 
$$(1/\xi^c)|\hat{\mathbf{g}}_{SU_1}\mathbf{w}_1^p|^2 + |\hat{\mathbf{g}}_{SU_1}\mathbf{w}_2^p|^2 + \sigma_1^2 \le f_1^{c,(\kappa)}(\mathbf{w}^c),$$
 (23b)  
 $(1/\xi^c)|\hat{\mathbf{g}}_{SU_2}\mathbf{w}_1^p|^2 + |\hat{\mathbf{g}}_{SU_2}\mathbf{w}_2^p|^2$ 

$$+\sigma_2^2 \le f_2^{c,(\kappa)}(\mathbf{w}^c),\tag{23c}$$

$$(1/\xi_1^p)|\hat{\mathbf{g}}_{SU_1}\mathbf{w}_2^p|^2 + \sigma_1^2 \le f_1^{p,(\kappa)}(\mathbf{w}_1^p), \tag{23d}$$

$$(1/\xi_2^p)|\hat{\mathbf{g}}_{SU_2}\mathbf{w}_1^p|^2 + \sigma_2^2 \le f_2^{p,(\kappa)}(\mathbf{w}_2^p),$$
 (23e)

$$\ln(1+1/\boldsymbol{\xi}^c) \ge \ln(1+1/\boldsymbol{\xi}^{c,(\kappa)}) + 1/(1+1/\boldsymbol{\xi}^c)$$

$$-\boldsymbol{\xi}^{c}/(\boldsymbol{\xi}^{c,(\kappa)}(1+\boldsymbol{\xi}^{c,(\kappa)})) \triangleq \boldsymbol{\mathcal{A}}^{c,(\kappa)}(\boldsymbol{\xi}^{c}), \tag{23f}$$

$$\ln(1+1/\boldsymbol{\xi}^p) \ge \ln(1+1/\boldsymbol{\xi}^{p,(\kappa)}) + 1/(1+1/\boldsymbol{\xi}^p) -\boldsymbol{\xi}^p/(\boldsymbol{\xi}^{p,(\kappa)}(1+\boldsymbol{\xi}^{p,(\kappa)})) \triangleq \boldsymbol{\mathcal{A}}^{p,(\kappa)}(\boldsymbol{\xi}^p),$$
(23)

$$-\boldsymbol{\xi}^{p}/(\boldsymbol{\xi}^{p,(\kappa)}(1+\boldsymbol{\xi}^{p,(\kappa)})) \stackrel{\triangle}{=} \boldsymbol{\mathcal{A}}^{p,(\kappa)}(\boldsymbol{\xi}^{p}), \qquad (23g)$$

$$\upsilon_{1} \geq \bar{\iota}_{1}, \qquad (23h)$$

$$v_1 \geq \frac{1}{2}$$
, (23i)

$$(19b), (19e),$$
 (23j)

where  $\boldsymbol{\xi}^{p} \in \{\xi_{1}^{p}, \xi_{2}^{p}\}, |\hat{\mathbf{g}}_{\mathrm{SU_{1}}}\mathbf{w}^{c}|^{2} \geq 2\Re\{(\hat{\mathbf{g}}_{\mathrm{SU_{1}}}\mathbf{w}^{c,(\kappa)})^{*}$   $(\hat{\mathbf{g}}_{\mathrm{SU_{1}}}\mathbf{w}^{c})\} - |\hat{\mathbf{g}}_{\mathrm{SU_{1}}}\mathbf{w}^{c,(\kappa)}|^{2} \triangleq f_{1}^{c,(\kappa)}(\mathbf{w}^{c}), |\hat{\mathbf{g}}_{\mathrm{SU_{2}}}\mathbf{w}^{c}|^{2} \geq 2\Re\{(\hat{\mathbf{g}}_{\mathrm{SU_{2}}}\mathbf{w}^{c,(\kappa)})^{*} (\hat{\mathbf{g}}_{\mathrm{SU_{2}}}\mathbf{w}^{c})\} - |\hat{\mathbf{g}}_{\mathrm{SU_{2}}}\mathbf{w}^{c,(\kappa)}|^{2} \triangleq f_{2}^{c,(\kappa)}(\mathbf{w}^{c}),$   $|\hat{\mathbf{g}}_{\mathrm{SU_{1}}}\mathbf{w}_{1}^{p}|^{2} \geq 2\Re\{(\hat{\mathbf{g}}_{\mathrm{SU_{1}}}\mathbf{w}_{1}^{p,(\kappa)})^{*} (\hat{\mathbf{g}}_{\mathrm{SU_{1}}}\mathbf{w}_{1}^{p})\} - |\hat{\mathbf{g}}_{\mathrm{SU_{1}}}\mathbf{w}_{1}^{p,(\kappa)}|^{2}$   $\triangleq f_{1}^{p,(\kappa)}(\mathbf{w}_{1}^{p}), \text{ and } |\hat{\mathbf{g}}_{\mathrm{SU_{2}}}\mathbf{w}_{2}^{p}|^{2} \geq 2\Re\{(\hat{\mathbf{g}}_{\mathrm{SU_{2}}}\mathbf{w}_{2}^{p,(\kappa)})^{*}$  $(\hat{\mathbf{g}}_{\mathrm{SU_{2}}}\mathbf{w}_{2}^{p})\} - |\hat{\mathbf{g}}_{\mathrm{SU_{2}}}\mathbf{w}_{2}^{p,(\kappa)}|^{2} \triangleq f_{2}^{p,(\kappa)}(\mathbf{w}_{2}^{p}).$ 

Consequently, problems (21) and (23) are addressed using an iterative approach that leverages the IA method, combined with a bisection search-based algorithm in steps 5-12, as detailed in Alg. 1.

To satisfy the discrete constraint on phase shifts, we apply a rounding function that maps the continuous phase shift

## Algorithm 1 : Proposed IA Algorithm to Solve Problem (19)

```
1: Initialization: Set (\mathbf{w}, \mathbf{\Phi}, \mathbf{\Psi}) := 0, generate an initial
      feasible point (\mathbf{w}^{(0)}, \boldsymbol{\xi}^{(0)}, \boldsymbol{v}^{(0)}) randomly, and relaxed \theta;
 2: Output: SEM and (\mathbf{w}^{\star}, \mathbf{\Phi}^{\star}, \mathbf{\Psi}^{\star}).
 3: Relaxed problem (19);
 4: repeat
         Initialize the lower \theta^{L} and upper \theta^{U} bounds of \theta;
 5:
         for l = 1, ...L do
 6:
             repeat
 7:
                 Calculate \theta^* = (\theta^{\mathsf{L}} + \theta^{\mathsf{U}})/2;
 8:
                 Update e^{j\theta_l}(\theta^*);
 9.
                 Calculate problem (21) to achieve \Phi^* and \Psi^*;
10:
             until Convergence
11:
         end for
12:
         Solve problem (23) to achieve (\mathbf{w}^{\star}, \boldsymbol{\xi}^{\star}, \boldsymbol{v}^{\star});
13:
14: until Convergence
15: Rounded \theta^* by using (24);
16: Calculate SEM in (19) based on (\mathbf{w}^{\star}, \mathbf{\Phi}^{\star}, \mathbf{\Psi}^{\star});
```

solution to its nearest valid discrete value as

$$\mathcal{A}(\theta) = \arg\min_{\varpi \in \mathcal{D}} |\theta - \varpi| \tag{24}$$

where  $\varpi$  is the rounding range. This step is necessary because, although the optimal phase shift solution is obtained, it remains in a continuous form and does not comply with the original discrete formulation.

#### IV. SIMULATION RESULTS

To evaluate the performance of the proposed algorithm in solving the formulated problem for multi-user STAR-RISassisted mMIMO-RSMA networks, we configure the simulation parameters as follows: The simulation area is set to  $200 \mathrm{m} \times 200 \mathrm{m} \times 200 \mathrm{m}$ , the target data rates for both users  $_{2}$  = 1bps/hz. The large scale fading is modeled as  $g_{\rm xy} = \mathcal{L}(d_{\rm xy}/d_0)^{-\sigma_{\rm PL}}$ . Here,  $\mathcal{L}$  denotes the path loss measured at the reference distance  $d_0$ ,  $d_0$  denotes the channel power at the reference distance d = 1m and  $d_{xy}$ represents distance between and which can be calculated as  $d_{xy} = \sqrt{(x_x - x_y)^2 + (y_x - y_y)^2 + (z_x - z_y)^2}$  and  $\sigma_{PL}$ denotes the path loss exponent [12]. The small-scale fading has i.i.d.  $\mathcal{CN} \sim$  The achieved result of SE in bit/sec/Hz, the SE in nat/sec/Hz is divided by ln(2). The convex optimization problem (23) is solved using the SDPT3 solver in conjunction with the YALMIP toolbox, implemented within the MATLAB environment [13].

Fig. 2 shows the impact of the maximum power budget at F-BS on the average SE. The average SE increases with higher  $\bar{P}_{BS}$ , as greater transmit power at the F-BS enhances the signal quality received by the ground users. Additionally, we compare our proposed algorithm against the exhaustive search (ES) algorithm as a benchmark scheme to demonstrate its effectiveness. The ES algorithm yields the highest SE performance, as it identifies the globally optimal solution by evaluating all possible configurations. The small performance gap between ES and Alg. 1 results from the

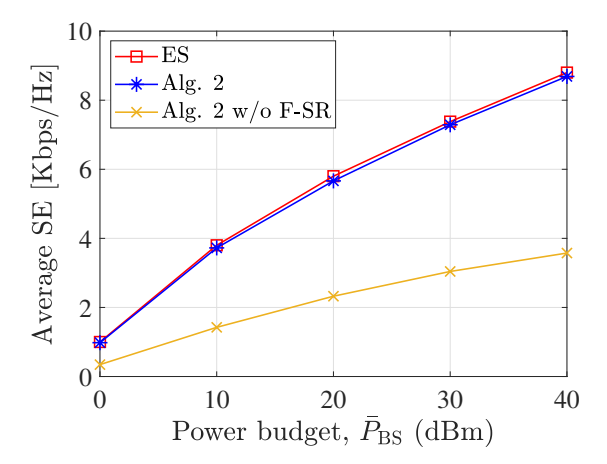


Fig. 2. Maximum power budget  $\bar{P}_{\mathrm{BS}}$  versus average SE.

relaxation of discrete phase shifts and the subsequent rounding in the proposed algorithm. Furthermore, the Alg. 1 without (w/o) F-SR performs the worst, as ground users receive signals only through the primary channel link (F-BS to ground users) without the additional signal contribution from the F-SR.

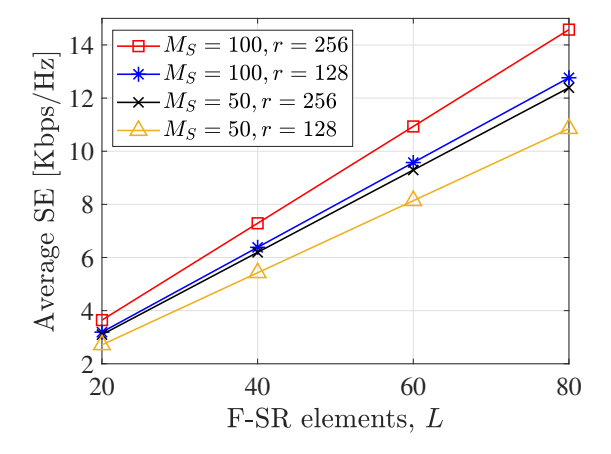


Fig. 3. Maximum F - SR elements L versus average SE.

Fig. 3 illustrates the impact of the number of F-SR elements on the average SE. As can be observed, the average SE increases with both the number of F-SR elements and the phase shift quantization levels due to the F-SR can more effectively control electromagnetic waves, focusing the incident signal from F-BS toward  $GU_1$  and  $GU_2$ . Additionally, increasing the number of F-BS antennas enhances the average SE performance by providing more degrees of freedom (DoF), which improves the system's beamforming and interference management capabilities.

#### V. CONCLUSIONS

In this paper, we studied a SEM problem in downlink aerial STAR-RIS-assisted mMIMO-RSMA networks. The formulated problem belonged to the class of non-convex mixed-

integer optimization due to the constraints on the maximum allowable portion of common SE, the power budget limitation at the F-BS, and the discrete phase shift configuration at the F-SR, making it challenging to solve optimally. To address this issue, we relaxed the original problem and decomposed it into two sub-problems: phase shift and beamforming, which were solved alternately. A bisection search method was employed to solve the phase shift sub-problem, while the IA technique was used to tackle the beamforming sub-problem by converting the non-convex formulation into a more tractable form. Simulation results demonstrated that the proposed scheme effectively improved SE performance. In addition, we evaluated the impact of the number of F-BS antennas and F-SR elements on the overall system performance. This paper lays the groundwork for future extensions that will incorporate deep learning techniques and consider satellite communication scenarios.

#### ACKNOWLEDGMENT

This research was supported by Basic Science Research Program through the National Research Foundation of Korea (NRF) funded by the Ministry of Education (RS-2023-00244014). This work was supported by Chungbuk National University BK21 program (2025).

#### REFERENCES

- [1] M. Na, J. Lee, G. Choi, T. Yu, J. Choi, J. Lee, and S. Bahk, "Operator's Perspective on 6G: 6G Services, Vision, and Spectrum," *IEEE Commun. Mag.*, vol. 62, no. 8, pp. 178–184, 2024.
- [2] R. H. Y. Perdana, T.-V. Nguyen, Y. Pramitarini, and B. An, "Deep Learning-Based Energy Efficiency Maximization in Massive MIMO-NOMA Networks With Multiple RISs," in 2024 Int. Conf. Artif. Intell. Inf. Commun. Osaka, Japan: IEEE, 2024, pp. 382–387.
- [3] M. Soleymani, I. Santamaria, and E. Jorswieck, "Energy-efficient Rate Splitting for MIMO STAR-RIS-assisted Broadcast Channels with I/Q Imbalance," in *Eur. Signal Process. Conf.* Helsinki, Finland: EURASIP, 2023, pp. 1504–1508.
- [4] R. H. Y. Perdana, T.-V. Nguyen, and B. An, "A Deep Learning-Based Spectral Efficiency Maximization in Multiple Users Multiple STAR-RISs Massive MIMO-NOMA Networks," in 2023 Twelfth Int. Conf. Ubiquitous Futur. Networks. Paris, France: IEEE, 2023, pp. 675–680.
- [5] J. Zheng, J. Zhang, H. Du, D. Niyato, D. I. Kim, and B. Ai, "Rate-Splitting for CF Massive MIMO Systems with Channel Aging," *IEEE Trans. Veh. Technol.*, vol. 73, no. 1, pp. 1485–1490, 2024.
- [6] X. Mu, Y. Liu, L. Guo, J. Lin, and R. Schober, "Simultaneously Transmitting and Reflecting (STAR) RIS Aided Wireless Communications," *IEEE Trans. Wirel. Commun.*, vol. 21, no. 5, pp. 3083–3098, 2022.
- [7] Y. Pramitarini, R. H. Y. Perdana, K. Shim, and B. An, "Secure Multicast Routing Against Collaborative Attacks in FANETs with CF-mMIMO and STAR-RIS: Blockchain and Federated Learning Design," *IEEE Internet Things J.*, vol. 12, no. 12, pp. 22404–22426, 2025.
- [8] R. H. Y. Perdana, T. V. Nguyen, Y. Pramitarini, K. Shim, and B. An, "Deep Learning-based Spectral Efficiency Maximization in Massive MIMO-NOMA Systems with STAR-RIS," in 2023 Int. Conf. Artif. Intell. Inf. Commun. Bali, Indonesia: IEEE, 2023, pp. 644–649.
- [9] D. Galappaththige and C. Tellambura, "Sum Rate Maximization for RSMA-Assisted CF mMIMO Networks With SWIPT Users," *IEEE Wirel. Commun. Lett.*, vol. 13, no. 5, pp. 1300–1304, 2024.
- [10] R. H. Y. Perdana, T. V. Nguyen, Y. Pramitarini, D. H. Nguyen, and B. An, "Enhancing Spectral Efficiency of Short-Packet Communications in STAR-RIS-Assisted SWIPT MIMO-NOMA Systems with Deep Learning," *IEEE Trans. Wirel. Commun.*, vol. 24, no. 1, pp. 842–859, 2025.
- [11] Q. Wu and R. Zhang, "Beamforming Optimization for Wireless Network Aided by Intelligent Reflecting Surface with Discrete Phase Shifts," *IEEE Trans. Commun.*, vol. 68, no. 3, pp. 1838–1851, Mar. 2020.

- [12] Y. Triwidyastuti, T. N. Do, R. H. Y. Perdana, K. Shim, and B. An, "Transfer Learning-Empowered Physical Layer Security in Aerial Reconfigurable Intelligent Surfaces-Based Mobile Networks," *IEEE Ac*cess, vol. 13, no. January, pp. 5471–5490, 2025.
- [13] R. H. Y. Perdana, T.-V. Nguyen, and B. An, "Adaptive User Pairing in Multi-IRS-aided Massive MIMO-NOMA Networks: Spectral Efficiency Maximization and Deep Learning Design," *IEEE Trans. Commun.*, vol. 71, no. 7, pp. 4377–4390, 2023.